Zeitschrift: IABSE reports = Rapports AIPC = IVBH Berichte

Band: 999 (1997)

Artikel: Strength and ductility of beam-to-column connections in hybrid bridge

Autor: Matsui, Shigeyuki / Ishizaki, Shigeru / Yukawa, Yasuyuki

DOI: https://doi.org/10.5169/seals-1013

Strength and Ductility of Beam-to-Column Connections in Hybrid Bridge

Shigeyuki MATSUI
Prof. Dr. of Civil Eng.
Osaka University
Osaka, Japan

Yasuyuki YUKAWA
Chief Struct. Engineer
Shikoku Branch of JH
Takamatsu, Japan

Nobuyoshi WADA
Struct. Engineer
Shikoku Branch of JH
Takamatsu, Japan

Shigeru ISHIZAKI
Manager
Sakai Iron Works Co., Ltd.
Osaka, Japan

Toshihiko TANAKA
Chief Struct. Engineer
Sakai Iron Works Co., Ltd.
Osaka, Japan

Summary

A new type of steel-concrete hybrid structure using a directly connecting method of steel girder to RC pier was employed to make the bridge behave as a structure. An elastic three dimensional finite element analysis and a static cyclic-loading test were carried out in order to confirm the ultimate strength and ductility of the connection. From those results, it was confirmed that the RC-type rigid connection employed herein is an excellent structural detail for beam-to-column connection in a hybrid rigid frame bridge.

1. Introduction

Recently in Japan, rigid frame type hybrid bridges consisting of steel girders and RC-piers have been adopted increasingly by reasons of structural simplicity and seismic advantage. In this type of bridges, it is important to design a durable and ductile structural detail for beam-to-column connections against temperature effect and earthquake.
RC-type rigid connection is a directly connecting method of steel main girder and RC pier. At the connecting section, cross beams are installed and many studs are provided on the girders and the cross beams to ensure the bond with concrete. In Okou Viaduct of Kochi-Highway in Japan, this type of connection was employed for the reasons of economical and aesthetical advantage and to obtain higher seismic resistance by increasing structural redundancy. However, until now, there is no practical construction using this type of rigid connection and the structural behaviors of the type are not clarified yet. Therefore, prior to actual construction, it is necessary to clarify the stress transfer mechanism, and to confirm the ultimate strength, the local behavior and failure, and the deformation capacity of the connection.
For the purpose mentioned above, an elastic three-dimensional finite element analysis for the connection using nonlinear joint spring elements at the interfaces of steel members and concrete was carried out. Moreover, a static cyclic loading test using a quarter scale specimen of the connection was also carried out. The paper describes the results of those analytical and experimental studies.

2. Structural Detail of Beam-to-Column Connection

The structural detail of RC-type rigid connection adopted herein is illustrated in *Fig. 1*. In this type of connection, among the stress resultant transferred from steel girder into RC pier, the major bending moment and normal force will be transferred, in the tension side of the column, mainly through the shear resistance of studs installed on the outside of web plate of the cross

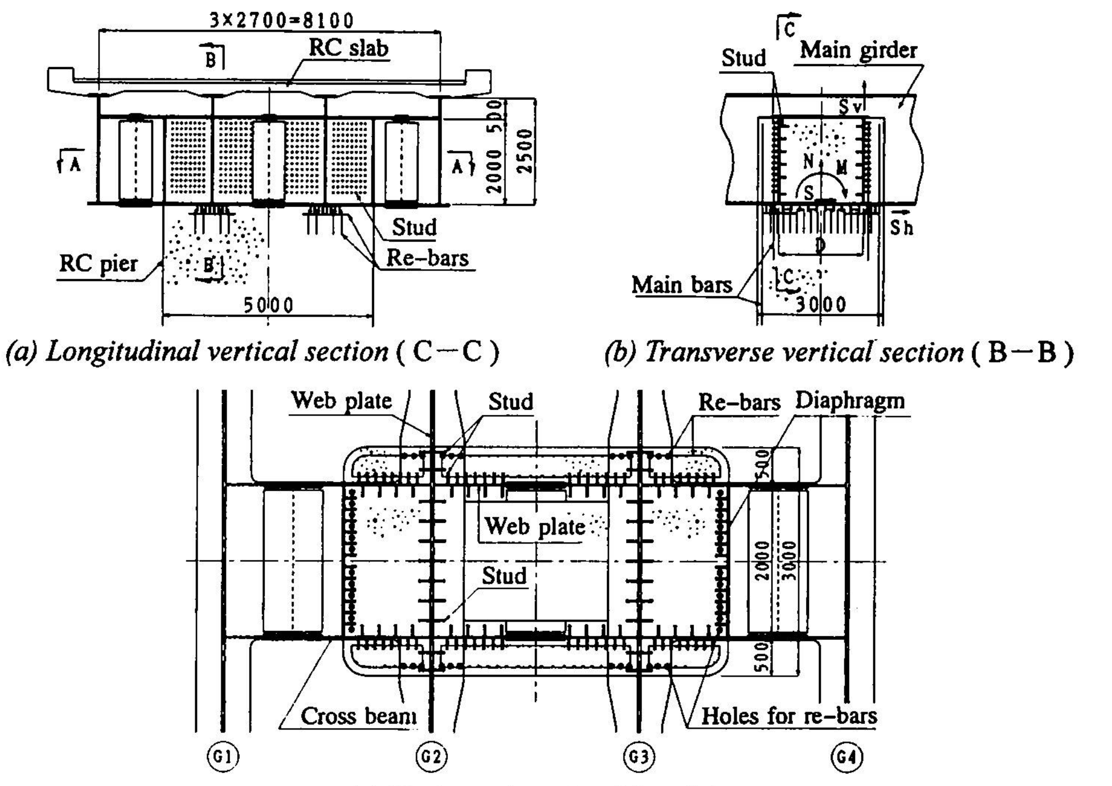

(a) Longitudinal vertical section (C—C) *(b) Transverse vertical section* (B—B)

(c) Horizontal section (A—A)

Fig. 1 Structural detail of beam-to-column connection

beam, and in the compression side, through both the shear resistance of the studs and the bearing resistance of concrete under the lower flange plate of main girders. Then the horizontal shear force will be transferred through the studs installed under the lower flange plate. Therefore, for the design of studs, it is assumed that the stress resultants from steel girders are transferred by the bearing resistance of the concrete under the lower flange and shear resistance of studs on the outside of cross beams and under the lower flange of main girder. Namely,

$$S_v = \frac{M}{D} - \frac{N}{2}, \quad \text{and} \quad S_h = S \tag{1}$$

where, S_v and S_h are the shearing forces acting on the studs on the outside of web plate of the cross beam in the tension side of the column and under the lower flange plates of main girders, respectively. M,N and S are the bending moment, axial force and shearing force acting on the column at the location of lower flange plate of main girders, respectively. *D* means the distance between two cross beams. In the connection, in order to transfer the shearing force smoothly to main reinforcing bars of RC pier through the studs, additional longitudinal reinforcing bars were arranged in front of the web plate of cross beams. Furthermore, the grillage reinforcement were also installed under the lower flange plate of main girders to softening the bearing stress.

3. FEM Analysis of the Connection

3.1 Analytical Model for FEM Analysis

In order to clarify the stress transfer mechanism at the beam-to-column connection through studs, an elastic three-dimensional finite element analysis for the connection was carried out with the meshing as shown in *Fig. 2.* The plate bending elements for steel girder members, the solid elements of hexahedra and pentahedra for concrete, and the nonlinear joint spring elements at the interface of steel elements and concrete were used as finite elements of the analysis. For the boundary condition of the analysis, the each three deformations and rotations with respect to x, y and z axes were fixed at the lower bound of the concrete column. The loading on the model was given by generating the stress resultants near the connection of analytical model being equal to those for the design earthquake load of the actual bridge. Furthermore, for the spring constant of shear spring element, the results of reference[1] were used in the analysis.

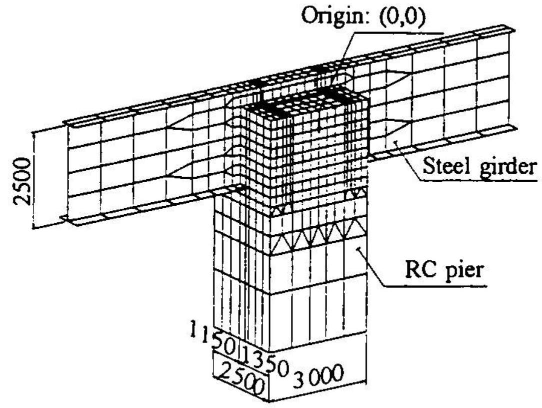

Fig. 2 Analytical model by FEM

3.2 Analytical Results and Considerations

Fig. 3 shows the distribution of shear force acting on the shear spring elements at the both outsides of web plates of the cross beams. From the figures, it can be seen that the shearing forces acting on the studs are developing larger value in the tension side than the compression side of the column. It can be considered because, in compression side, the forces from main girders are mainly resisted by the bearing of the concrete under the lower flange plate of steel girder. The shearing force per unit area given by eq.(1) is about 130tf/m^2, which is over the double of the mean value 50tf/m^2 obtained by FEM analysis. It can be explained due to the pull out resistance of studs under the lower flange plate of main girder, the bearing resistance of concrete over the flange plate, and the shear resistance of studs on the web plates of main girders

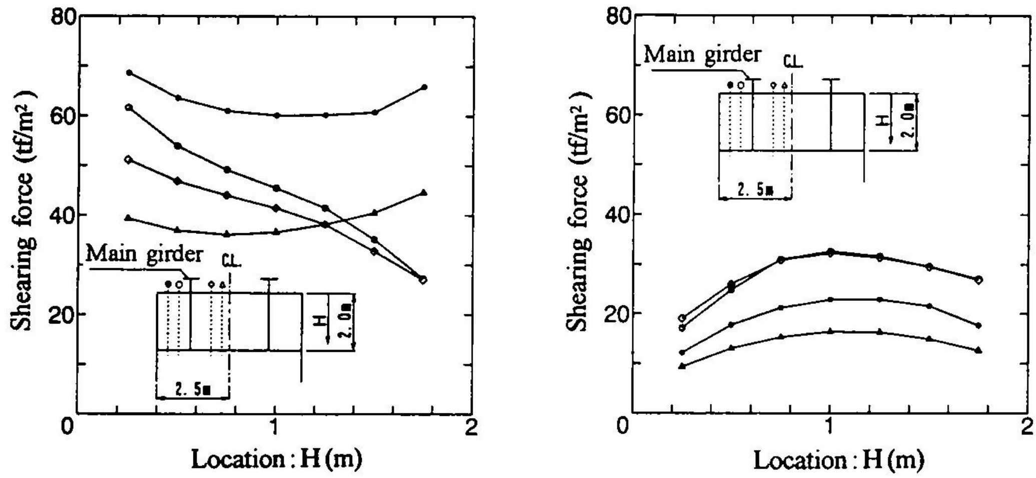

a) Tension side *b) Compression side*

Fig. 3 Stress distribution of shear acting on studs at the outside of web plate of cross beam

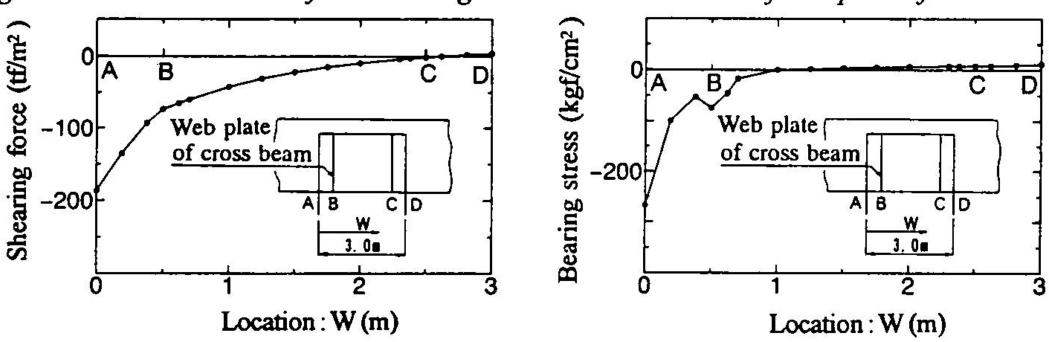

a) Shear stress of studs *b) Bearing stress of concrete*

Fig. 4 Shear force distribution of studs and bearing stress distribution of concrete under the lower flange plate of main girder, respectively.

are contributing for the transmission of the resultant force in the tension side of the column. However, the eq.(1) was used for the design of studs considering that the shear strengths of studs are scattered depending on the state of the filling concrete and the shearing forces acting on studs are also scattered depending on the location. *Fig. 4* shows the distribution of the horizontal shear and the bearing stress under the lower flange plate of main girder along the web line. From the figure, it can be seen that both the shear and bearing stress acting under the flange concentrate in the edge of compression side of the column. Therefore, additional reinforcements should be installed to softening the bearing stress.

4. Static Cyclic Loading Test of Beam-to-Column Connection

4.1 Test Specimen

A quarter scale specimen of the connection with RC pier and a pair of steel main girders was employed and the specimen was installed upside down for the actual bridge from the restriction of loading equipment as shown in *Fig. 5*. Therefore, the upside-down expressions against the actual bridge are used hereafter. Moreover, the cross sectional dimensions of steel beams and the arrangement and diameter of reinforcing bars in the column were also determined to coincide with the yield moment of the complete quarter scale sections of actual bridge. The dimensions and the material properties of the specimen are shown in Table-1.

Table 1 Dimensions and material properties of the specimen

Dimensions of specimen (mm)				Yield Point (N/mm^2)	Young's Moduli (N/mm^2)
Steel Girder	Main Girder	Flange	150 x12	283	212000
		Web	625 x 9	293	211000
	Cross Beam	Flange	500 x 4.5	—	—
		Web	80 x 4.5	—	—
RC-Column	Re-bar	Main bar	D13	448	211000
		Hoop bar	D6	416	212000
	Concrete		1250x750	—	16600
Stud dowel			ϕ 13x65	—	

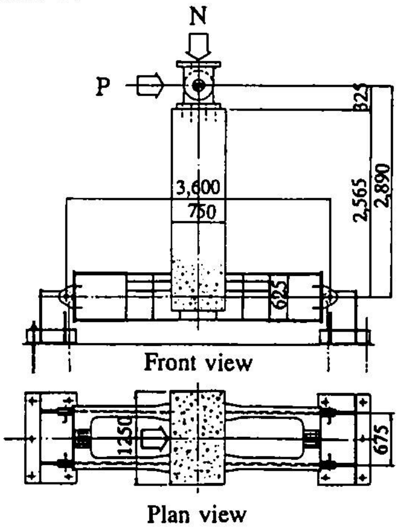

Fig. 5 General dimensions of specimen

4.2 Loading Procedure

The axial compressive load was kept in constant by vertical hydraulic actuator, while the horizontal cyclic loading was being applied simultaneously by another hydraulic jack to reproduce the same distribution of the stress resultant in the connection as actual bridge. The applied axial load was determined to give the same stresses in the specimen as the stresses in actual bridge due to dead load. Load was applied by load control method up to the initial yielding load of main bars, thereafter, displacement control method using multiples of the yielding displacement δ_y, was used. The yielding of reinforcing bar was judged by the shape of *P*- δ curve and the measured strain of main reinforcements.

4.3 Test Results and Considerations

4.3.1 Ultimate strength and deformation capacity of beam-to-column connection

A hysteretic curve of horizontal load versus horizontal displacement is shown in *Fig. 6*. In this experiment, the incremental displacement after yielding of reinforcements was defined by the multiples of measured initial yielding displacement δ_y. However, the displacement includes the movement of support and the displacement due to rigid body rotation of steel girder, so that the measured displacement takes apparently large value. Therefore, the revised displacement are

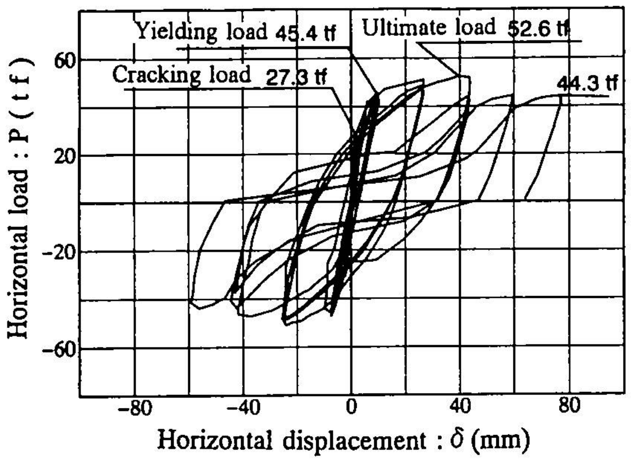

Fig. 6. Hysteretic curve of horizontal load versus displacement

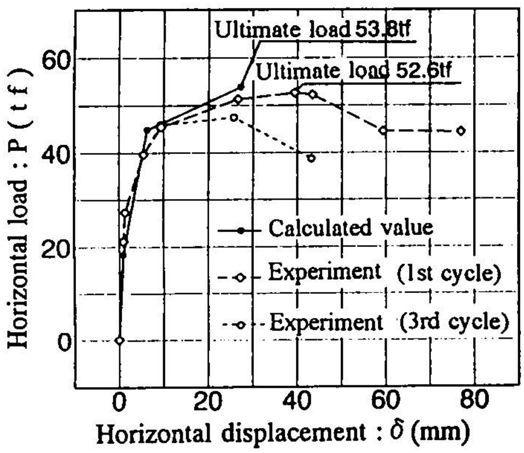

Fig. 7 Envelope of horizontal load versus displacement

Table 2 Multiples for yield displacement

Displacement (mm)	Measured	17.5	35.7	53.1	68.0	85.6
	Revised	9.4	26.6	43.4	59.4	77.0
Revised multiple number		1.0	2.8	4.6	6.3	8.2

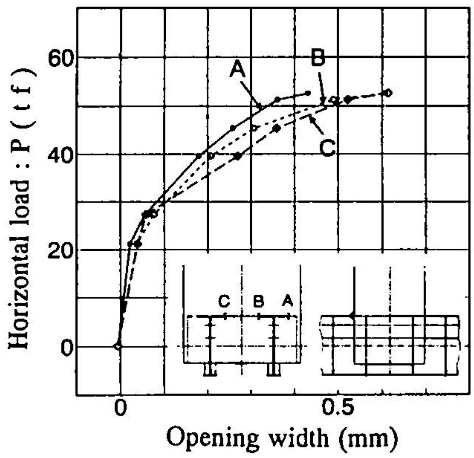

Fig.8 Opening at the contact surface of flange plates and concrete

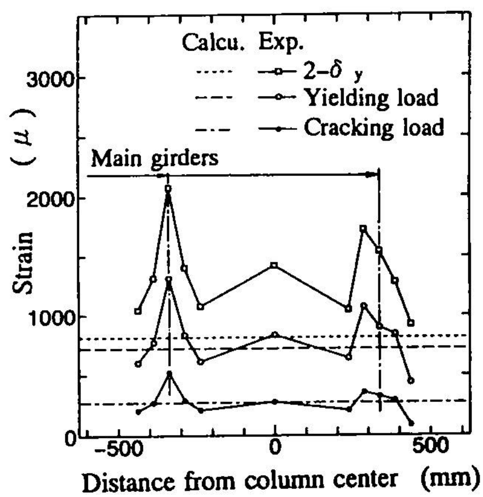

Fig.9 Strain distribution of concrete

used in *Fig. 6.* The multiple number of displacement based on revised yield displacement is shown in *Table. 2.* From these figure and table, it can be seen that the displacement for the maximum load is 4.2 times as large as δ_y and the specimen has the remaining capacity of 84% of the maximum load for the displacement of 8.2 times as large as initial yield displacement. *Fig. 7* shows the envelopes of the 1st and 3rd cycle of loading compared with a calculated value based on reference [2].

From this figure, it can be seen that, before the yielding of reinforcing bars, there is no significant difference between 1st and 3rd cycles of P- δ relation. However, after yielding of reinforcing bars, the load carrying capacity for 3rd cycle was considerably decreased comparing with that of 1st cycle. This is considered to be due to the developing of plastic region in the main reinforcements of RC column by cyclic loading. The experimental ultimate load was well agreed with the calculated one.

4.3.2 Opening between flange plate and concrete

The relationship between horizontal load and opening width of contacting surface between flange plate of main girder and concrete are shown in *Fig. 8.* Though the opening was relatively small (maximum value of 0.08mm) for the load not exceeding the cracking load of 27.3tf, thereafter, the opening rapidly increased. The maximum opening of 0.61mm was observed at the maximum load. However, for the double of design earthquake load of 21.2tf, the opening was about 0.2 mm, and no injurious cracks were observed.

4.3.3 Strain at the surface of concrete
Fig. 9 shows the distribution of compressive strain on the column face at the flange level of main girders for each loading level. The calculating value shown in the figure are given under the assumption of RC section ignoring tension side of concrete, and the additional longitudinal reinforcement in front of cross beams, are also taking into account in the moduli of RC section. From the figure, the bearing strain concentration can be observed over the web plate of main girder, and the test results for the cracking load was 1.9 times as large as calculating value. However, even when the final failure of specimen, any crashing of concrete at the portion was not recognized. From the fact, it can be considered that the grillage reinforcements arranged over the lower flange plate in order to softening the bearing stress worked effectively.

4.3.4 Development of cracks and failure mode
The first crack in concrete of the specimen was observed at the cross section upside 50cm from the flange plate at the loading of 27.3 tf. The location was coincident with the terminating point of additional reinforcing bars installed in front of the web plate of cross beam. Thereafter, until the horizontal load reaches 40-tf, cracks developed and widely spread with the increase of loading. However, for the load over 40-tf, though the increase of crack width was observed, new cracks didn't occurred. The first failure occurred in concrete at the compression side of the column. The failure mode was the spalling of covering concrete with the buckling of main reinforcement as shown in *Fig. 10*. Thereafter, the concrete crushing has developed to inside of reinforcing bars with the increase of loading. However, the column concrete in the connecting part has remained in sufficiently sound at the final failure state of RC column. From the fact, it can be confirmed that the combination of the studs on the outside of the cross beams, the additional reinforcements in front of them, the main reinforcement of the column, and the hoop reinforcements enclosed these reinforcements worked effectively.

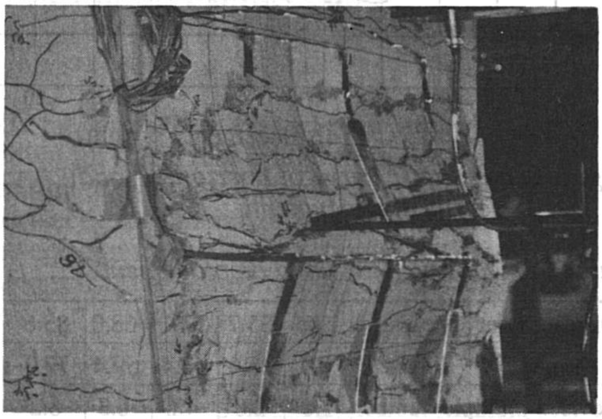
Fig. 10 Spalling-off of covering concrete

5. Conclusions

From the results of analytical and experimental studies mentioned above, the conclusions can be summarized as follows;
(1)The concrete at the connecting part was completely sound for both the principal design loads and the design earthquake load. The final failure occurred at RC column, even then the steel girder and RC pier were rigidly connected by studs.
(2)For the displacement of 8.2 times of the initial yielding displacement, the specimen has shown the remaining capacity of 84% of the maximum load carrying capacity. Therefore, it can be considered that the connection has enough ductility.
(3)The bearing strain concentration was recognized at the edge concrete of the column under the contact surface between lower flange plate of main girder and concrete. However, even when the final failure of specimen, no local failure was recognized at the part, and the connection was completely sound. From the fact, the efficacy of strengthening method adopted herein were confirmed.

References

[1] Matsuda, T., et al. : Structural Behavior of Connection between Steel Girder and RC One Using Studs, Proc. of the 50-th Annual Meeting of JSCE, I-124, Sept. 1995. (in Japanese)
[2] Japan Road Association : Reference for applying the "Tentative Specifications for Restoration of Damaged Highway Bridges by Southern Hyogo Earthquake", Feb. 1995. (in Japanese)